Analysis of Electrodes for Body-Centric Communications

[#]Nozomi Haga [1], Kazuyuki Saito [1], Masaharu Takahashi [1], Koichi Ito [1]
[1] Chiba University
1-33 Yayoi-cho, Inage-ku, Chiba 263-8522, Japan, n_haga@graduate.chiba-u.jp

1. Introduction

In recent years, antennas and propagation for body-centric wireless communications have become an active area of research because of their various applications [1]–[5]. Whereas on-body communications at microwave frequency bands have widely been investigated especially in Europe, communications using low-frequency bands are also in researches' and corporations' interest especially in Japan [2]–[4]. In previous studies, the signal transmission mechanism was investigated by using numerical simulations and experiment [3]. In addition, equivalent circuit model of transmission channel was introduced [4]. However, there have been few reports in terms of operation mechanism and optimization of electrodes. In this study, we have numerically conducted some parameter studies to understand fundamental characteristics of the electrodes.

2. Model and Methods of Numerical Analysis

In our previous study, it has been clarified that the on-body channel is flat independently of frequency below several tens of megahertz [5]. This fact implies that the quasi-static approximation is applicable in these frequencies, and that the electric stored energy is an important index of communication performance. For these reasons, we have numerically analyzed electrostatic characteristics of the electrodes. Fig. 1 shows a numerical analytical model, which includes parallel-plate electrodes and a conducting sphere which represents human head. The electrodes have a square shape of $L \times L$ and zero thickness, and are separated by a gap d_1. Diameter of the conducting sphere is 200 mm. The bottom electrode and the sphere are separated by a gap d_2. The origin of coordinate is set to be center of the sphere. Incidentally, we have already confirmed that even if the sphere is represented by lossy dielectrics comparable to muscle, the electric field generated around the sphere remains constant up to about 30–40 MHz. For instance, the received open voltage of a receiving electrodes equipped at the opposite side of the sphere, is plotted in Fig. 2. Discrepancy between the time-varying voltage and the static asymptote is within 0.5 dB below 58 MHz.

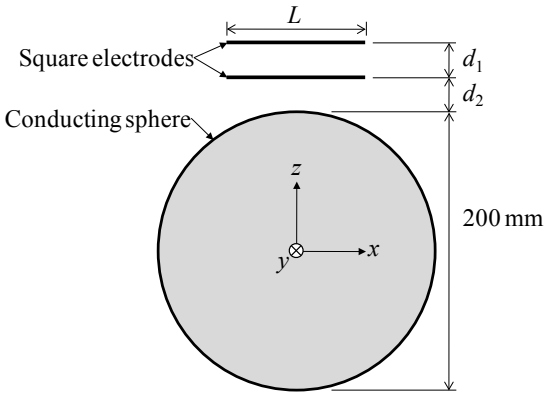

Figure 1: Numerical Analytical Model.

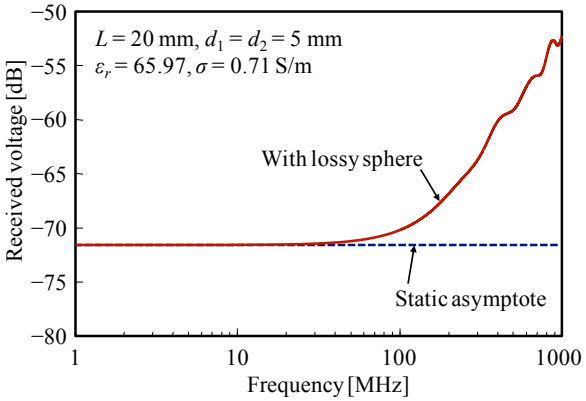

Figure 2: Applicable Range of Analysis

In order to ensure the reliability of the results, we employed two different methods, namely, the boundary element method (BEM) and the finite-difference time-domain (FDTD) method. In the BEM, time variation of the electromagnetic field is essentially ignored. In other words, only the Gauss' law is considered. The electrodes are divided into 80 × 80 segments. The surface charge density σ is assumed to be constant on each segment. Instead of dividing the sphere into segments, we used a Green's function G that satisfy a boundary condition $G = 0$ on the surface of the sphere

$$G(\boldsymbol{r},\boldsymbol{r}') = \frac{1}{4\pi|\boldsymbol{r}-\boldsymbol{r}'|} - \frac{1}{4\pi|\boldsymbol{r}-\boldsymbol{r}''||\boldsymbol{r}'|}\frac{a}{} \tag{1}$$

where $\boldsymbol{r}$ is the observation point, $\boldsymbol{r}'$ is the source point, a is the radius of the conducting sphere, and $\boldsymbol{r}''$ is the position of the image source

$$\boldsymbol{r}'' = \frac{a^2}{|\boldsymbol{r}'|^2}\boldsymbol{r}' \tag{2}$$

If the given potential on the sphere ϕ_{sphere} is not zero, an additional point charge can be assumed in the center of the sphere so as to satisfy the given boundary condition. Therefore, the integral equation to be solved is as follows.

$$\phi(\boldsymbol{r}) - \frac{a}{|\boldsymbol{r}|}\phi_{sphere} = \frac{1}{\varepsilon_0}\iint_S G(\boldsymbol{r},\boldsymbol{r}')\cdot\sigma(\boldsymbol{r}')d\boldsymbol{r}' \tag{3}$$

where ε_0 is the permittivity of vacuum, and S is the surface region of the electrodes. For the linearity of the system, potential and charge distributions on the electrodes when net charges of each conductor are specified can easily be obtained. For example, to calculate the capacitance between the electrodes, net charges on the electrodes and the sphere are set to be ±1 C and 0 C, respectively.

In the FDTD analysis, the static characteristics can theoretically be obtained by using the Fourier transformation. However, we have to be attentive to precision of the absorbing boundary condition and undesired reflections from the boundary. For the perfectly matched layer (PML) absorbing medium, as the number of the layers increases, reflections back toward analytical region are suppressed for lower frequency. This means that the reflected waves in the time domain rise slower for larger number of the PML. Therefore, the reflected waves can be excluded with a large enough number of the PML and an appropriate time gate. In the present case, 20-layer PML surrounds the free-space region of 400 mm × 400 mm × 400 mm. The minimum mesh divides the electrodes into 80 × 80 segments (e.g., 0.25 mm for L = 20 mm and 1mm for L = 80 mm). The conducting sphere is approximated by using 1-mm staircasing. Size of the maximum mesh adjacent to the PML is 5 mm. The electrodes are fed at its center by a current source of which length is d_1. Exciting waveform is a derivative Gaussian pulse of which spectrum is−6 0 dB at 1 GHz. The iterative calculation was terminated before reflections appear (e.g., 19.2 ns for L = 20 mm).

3. Results and Discussion

3.1 Capacitance between Electrodes

As described earlier, we believe that electric energy stored around the human body is an important index of low-frequency communications. In order to quantify the energy stored around the conducting sphere, we conceptually divide the capacitance between the electrodes into two components as described below. In principle, capacitance C between two conductors with charges $\pm Q$ and potential difference V are defined as $C = Q/V$. In addition, amount of the electrostatic energy U is given by $U = CV^2/2$. Therefore, the capacitance can be expressed in terms of U and V.

$$C = 2\frac{U}{V^2} \tag{4}$$

Besides, energy stored in a region between the electrodes U_{inside} can be calculated from a volume integral of the electric field, and energy stored outside the electrodes is the difference of U from U_{inside}. Therefore, using U_{inside} and $U_{outside}$, we can define the inside and outside region component of the capacitance C_{inside} and $C_{outside}$. For larger $C_{outside}$, the magnitude of the electric field generated around the sphere can be greater.

Fig. 3 plots respective components of the capacitance between the electrodes as functions of the side length L. The solid lines and the symbols indicate the results obtained with the BEM and the FDTD, respectively. In addition, the broken line indicates the capacitance calculated with an approximate formula $C \approx \varepsilon_0 L^2/d_1$. The total capacitance is always greater than the approximate value, and the inside region component almost agrees with the approximation. The outside region component linearly increases with L. Fig. 4 plots the capacitances as functions of the distance between the electrodes d_1.Whereas the inside region component is inversely proportional to d_1, the outside region component does not vary so much. Fig. 5 plots the capacitances as functions of the distance between the bottom electrode and the sphere d_2. The outside region component somewhat increases as d_2 gets smaller. In other words, the capacity of energy storage is increased by the presence of the sphere. According to these results, it can be concluded that the side length of electrodes is the most effective parameter for the outside region component. This fact will be important in designing transmitters.

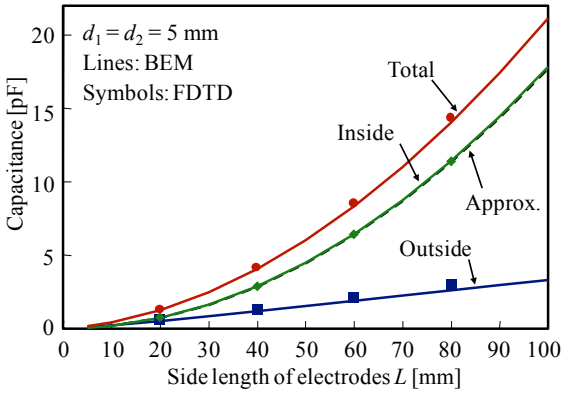

Figure 3: Capacitance due to L

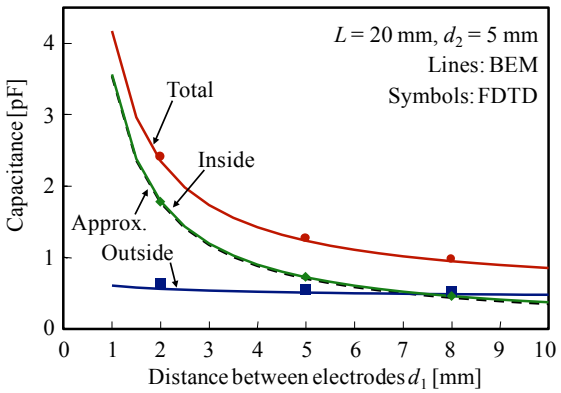

Figure 4: Capacitance due to d_1

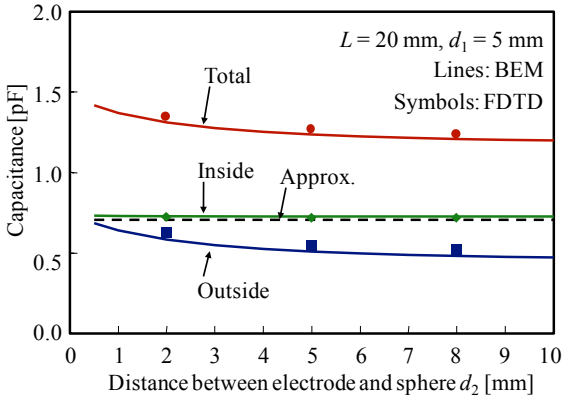

Figure 5: Capacitance due to d_2

3.2 Received Open Voltage

In order to assess the electrodes as a receiver, open voltage between the electrodes with zero net charge was calculated by using the BEM. The conducting sphere is charged so as to be 1 V in potential. As shown in Fig. 6, the received open voltage decreases with increasing L. That is because negative charges tend to converge at the center of the electrodes for larger L (see Fig. 7). Fig. 8 plots the received open voltage as a function of d_1. The voltage naturally increases linearly with d_1. Fig. 9 plots the received open voltage as a function of d_2. The voltage gently decreases with d_2. According to these results, it can be summarized that the distance between electrodes is the most effective parameter for receiving voltage, and that oversized electrodes may decrease the receiving efficiency.

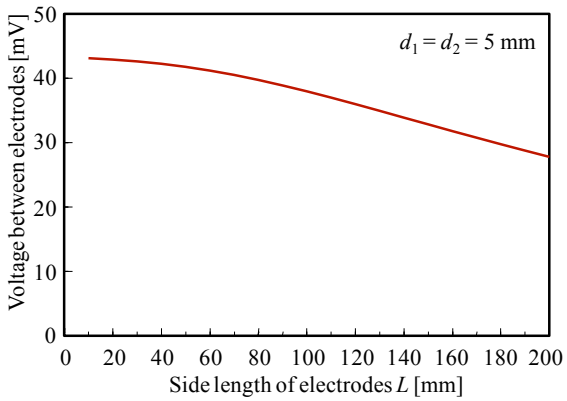

Figure 6: Received Voltage due to L

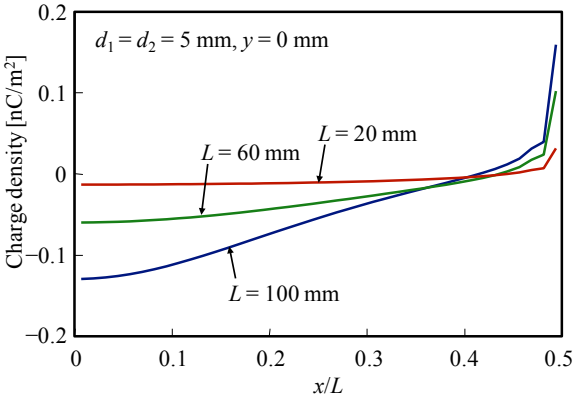

Figure 7: Charge Density on Bottom Electrode

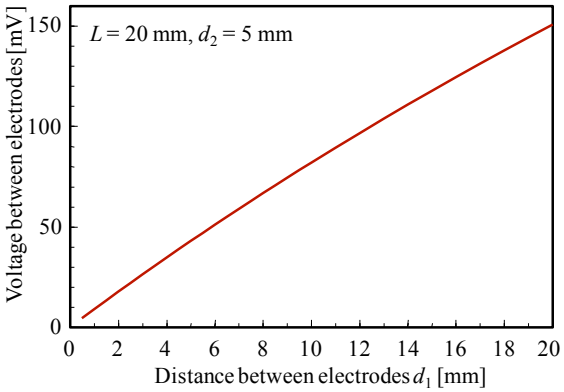

Figure 8: Received Voltage due to d_1

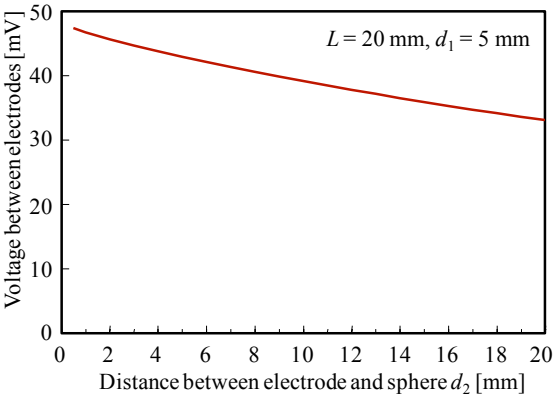

Figure 9: Received Voltage due to d_2

4. Conclusion

In the present paper, capacitances and received voltages of parallel-plate electrodes in vicinity of a conducting sphere was numerically calculated with various parameters. According to the results, the side length of the electrodes is the most effective parameter for outside region component of capacitance and the amount of the outside region component is linearly proportional to the side length. Furthermore, the received voltage is proportional to the distance between the electrodes, and oversized electrodes may decrease the received voltage. In the further study, we will address to optimize the electrodes based on the present results.

References

[1] Special Issue on "Antennas and Propagation for Body-Centric Wireless Communications", *IEEE Trans. Antennas Propag.*, March 2009.

[2] http://www.redtacton.com/

[3] K. Fujii, M. Takahashi, and K. Ito, "Electric field distributions of wearable devices using the human body as a transmission channel," *IEEE Trans Antennas Propag.*, vol. 55, no. 7, pp. 2080–2087, Jul. 2007.

[4] K. Hachisuka, *et al.*, "Simplified circuit modeling and fabrication of intrabody communication devices," *Sensors and Actuators A Physical*, A130–131, pp.332-330, Apr. 2006.

[5] N. Haga and K. Ito "Frequency dependence of on-body channels with top-loaded monopole antennas in the range of HF to UHF," in *Proc of Asia-Pacific Microwave Conference 2009*, pp. 2208–2211, Singapore, Dec. 2009.